

Accepted Article

Title: Encapsulation of Homogeneous Catalysts in Mesoporous Materials Using Diffusion-Limited Atomic Layer Deposition

Authors: Shufang Zhang, Bin Zhang, Haojie Liang, Yequn Liu, Yan Qiao, and Yong Qin

This manuscript has been accepted after peer review and appears as an Accepted Article online prior to editing, proofing, and formal publication of the final Version of Record (VoR). This work is currently citable by using the Digital Object Identifier (DOI) given below. The VoR will be published online in Early View as soon as possible and may be different to this Accepted Article as a result of editing. Readers should obtain the VoR from the journal website shown below when it is published to ensure accuracy of information. The authors are responsible for the content of this Accepted Article.

To be cited as: *Angew. Chem. Int. Ed.* 10.1002/anie.201712010
Angew. Chem. 10.1002/ange.201712010

Link to VoR: <http://dx.doi.org/10.1002/anie.201712010>
<http://dx.doi.org/10.1002/ange.201712010>

Encapsulation of Homogeneous Catalysts in Mesoporous Materials Using Diffusion-Limited Atomic Layer Deposition

Shufang Zhang,^[a,b] Bin Zhang,^{*[a]} Haojie Liang,^[a,b] Yequn Liu,^[a] Yan Qiao,^[a] Yong Qin^{*[a]}

Abstract: The heterogenization of homogeneous metal complex catalysts has attracted great attention. Herein, we report the encapsulation of metal complexes into nanochannels of mesoporous materials by coating metal oxides at/near the pore entrance via diffusion-limited atomic layer deposition (ALD) to produce a “hollow plug”. The pore size of the hollow plug is precisely controlled on the sub-nanometer scale by the number of ALD cycles to fit various metal complexes with different molecular sizes. Typically, Co or Ti complexes are successfully encapsulated into the nanochannels of SBA-15, SBA-16 and MCM-41. The encapsulated Co and Ti catalysts show excellent catalytic activity and reusability in the hydrolytic kinetic resolution of epoxides and asymmetric cyanosilylation of carbonyl compounds, respectively. This ALD-assisted encapsulation method can be extended to the encapsulation of other homogeneous catalysts into different mesoporous materials for various heterogeneous reactions.

Chemical reactions can be confined to a nano-space by encapsulating catalysts in nanoreactors.^[1] In past decades, researchers have focused much effort into the development of nanoreactors for various applications in cell biology, tissue engineering, medical diagnostics and therapies, and catalysis.^[2] Among a series of nanoreactors, porous materials provide a uniform and stable nanochannel to immobilize catalysts.^[3] Compared to the immobilization of metal complexes in porous materials by chemical bonds, the encapsulation of metal complexes via physical adsorption in the pore channels is preferred since the properties and freedom of metal complexes are similar to those of homogeneous catalysts, which leads to the advantages of both homogeneous and heterogeneous catalysts.^[4]

The “ship in a bottle” method^[5] and enclosing catalysts by non-covalently bonding^[6] are two typical strategies to encapsulate metal complexes into ordered porous materials. For the “ship in a bottle” method, the microporous zeolite structure limits the molecular size and freedom of the catalysts and even the diffusion of reactants. To solve these problems, Li and coworkers have developed a method to encapsulate metal complexes into cage-like mesoporous materials (SBA-16 and

FDU-12) by reducing the size of the pore entrance to molecular scale via silylation.^[7] Compared to SBA-16 and FDU-12, the cylinder-like mesoporous materials (such as SBA-15 and MCM-41) are more superior in mass and heat transfer.^[8] However, it is a great challenge to encapsulate the metal complexes into cylinder-like mesoporous materials by silylation, and no other chemical method has been developed because the reagents for encapsulation can easily diffuse into the mesopore channels in the solution system, and the size of the silylating agents matching the large pore entrance is limited.^[4a] Therefore, it is desirable to develop highly efficient methods to precisely modify the large pore entrance of cylinder-like mesoporous materials on a sub-nanometer scale to encapsulate metal complexes with different molecular sizes.

Atomic layer deposition (ALD) is a cyclic process for the sequential self-limiting chemical reaction between precursor molecules and a solid surface.^[9] The self-limiting nature of ALD assures its distinctive and unique advantages in precise film thickness control and excellent coverage, even in 3D porous materials.^[10] Recently, using ALD, our group has synthesized a series of highly efficient catalysts with distinctive structures,^[11] which demonstrated greatly enhanced activity and stability by optimizing the metal-oxide interface.

Herein, we report a highly efficient and general method to encapsulate metal complexes into straight nanochannels by reducing their pore sizes only at/near the pore entrance by diffusion-limited ALD. The limited diffusion depth due to the short diffusion time of the precursors results in a “hollow plug” at the pore entrance (Scheme 1). Moreover, the pore size of the hollow plug could be precisely controlled by the ALD cycle numbers. We successfully encapsulated [(R,R)-N,N'-Bis(3,5-di-*tert*-butylsalicylidene)-1,2-cyclohexanediamine]Co(III) (Co(salen)) and [(R,R)-N,N'-bis(3,5-di-*tert*-butylsalicylidene)-1,2-cyclohexanediamine]Ti(μ-O)₂ [(salen)Ti(μ-O)₂] complexes into SBA-15, SBA-16, and MCM-41. The encapsulated catalysts show excellent catalytic activity and stability in the hydrolytic kinetic resolution (HKR) of epoxides and the asymmetric cyanosilylation of carbonyl compounds, respectively.

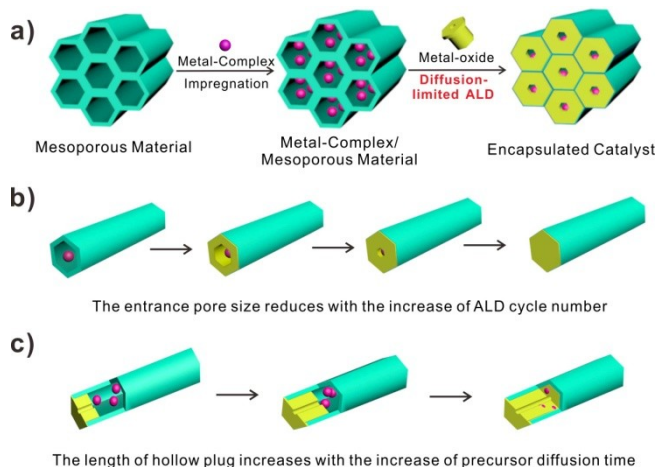
Scheme 1 illustrates the process of encapsulating metal complexes into the channels of mesoporous materials, with SBA-15 as an example. Co(salen) was first introduced into the nanochannels of SBA-15 with the most probable pore size of 9.2 nm (Figure S1) (denoted as Co(salen)/SBA-15) by the vacuum impregnation method^[7a] (see supporting information, Methods). Subsequently, a TiO₂ film was deposited by ALD at 45 °C into the pores of SBA-15 using titanium tetraisopropoxide (TIP) and H₂O as precursors. The low temperature was applied to avoid the deterioration of chirality of Co(salen). The pulse, exposure, and purge times for TIP were 0.5, 1, 120 s, respectively, and for H₂O were 0.1, 8, 120 s, respectively. The long purge time was applied to avoid chemical vapor deposition due to the low deposition temperature.^[12] The short total diffusion time (t = 1.5 s,

[a] Shufang Zhang, Bin Zhang, Haojie Liang, Yequn Liu, Yan Qiao, Yong Qin
State Key Laboratory of Coal Conversion, Institute of Coal Chemistry, Chinese Academy of Sciences
Taiyuan 030001, PR China
E-mail: zhangbin2009@sxicc.ac.cn, qinyong@sxicc.ac.cn

[b] Shufang Zhang, Haojie Liang
University of Chinese Academy of Sciences
Beijing 100039, PR China

Supporting information for this article is given via a link at the end of the document.

pulse plus exposure time) for TIP was used to ensure the deposition of TiO_2 only at/near the pore entrance of SBA-15. The pore size at pore entrance was gradually reduced from the initial 9.2 nm to the molecule size of the metal complexes (~ 0.8 nm)^[13] by increasing the number of TiO_2 ALD cycle (m). Finally, the samples were washed in tetrahydrofuran (THF) three times to obtain the encapsulated catalysts, denoted as $m\text{TiO}_2\text{-t/Co(salen)/SBA-15}$.



Scheme 1. (a) Schematic illustration of the encapsulating process of metal-complexes into ordered mesoporous materials. (b) Increase of ALD cycle number to reduce the pore size. (c) Increase of diffusion time of precursor to increase the length of the hollow plugs.

Figure 1a and Figure S2 show a scanning electron microscope (SEM) image of the original SBA-15 samples with a channel length ranging from 2 to 50 μm . Figures 1b and 1c show the transmission electron microscope (TEM) images of SBA-15 before and after encapsulation of Co(salen) , respectively. The darker contrast indicates that TiO_2 is successfully deposited in the channels of SBA-15 after 200 ALD cycles ($200\text{TiO}_2\text{-1.5/Co(salen)/SBA-15}$). The ordered pore structure of SBA-15 was maintained after TiO_2 ALD, which is consistent with the small-angle X-ray diffraction results (Figure S3). Figure 1d shows the TEM image projected with the electron beam parallel to the channels of SBA-15 after TiO_2 ALD. A tubular TiO_2 film with darker contrast is clearly visible at the pore entrance, and the pore size decreased to approximately 0.8 nm, which is similar to the molecular size of Co(salen) . The growth rate of TiO_2 ALD was measured by TEM analysis of the carbon nanofibers coated with TiO_2 under the same conditions (Figure S4). According to the determined growth rate of 0.025 nm per cycle, the reduced pore size of 8.4 nm (9.2-0.8 nm) corresponds well to the expected filled pore size of approximately 10 nm (two times the thickness of the deposited TiO_2 film), considering that the substrate has slight influence on the growth rate of the ALD film. From the energy dispersive X-ray spectroscopy (EDX) mapping (Figure 1e), the deposition depth (length of the plug) of TiO_2 was found to be approximately 1.1 μm . Further, the deposition depth is revealed by (scanning transmission electron microscope (STEM) image and EDX mapping (Figure 1f) of a

cross-sectional specimen prepared by focused ion beam (FIB) milling along the axis of the SBA-15 channels. Moreover, the ^{13}C cross polarization magic angle spinning nuclear magnetic resonance spectra (^{13}C CP/MAS NMR) show that the peaks corresponding to the $200\text{TiO}_2\text{-1.5/Co(salen)/SBA-15}$ are identical to those of Co(salen) (Figure S5). These results reveal that Co(salen) was successfully encapsulated in SBA-15.

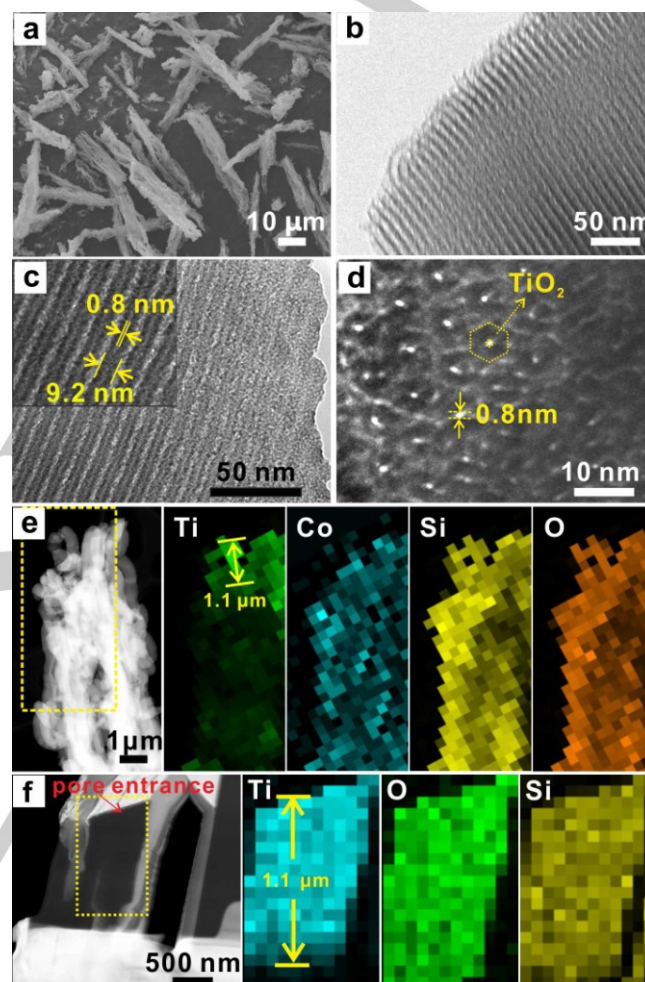


Figure 1. (a) SEM image and (b) TEM image of SBA-15; (c) and (d) HRTEM images of encapsulated catalyst $200\text{TiO}_2\text{-1.5/Co(salen)/SBA-15}$; (e) STEM image and EDX mapping of encapsulated catalyst $200\text{TiO}_2\text{-1.5/Co(salen)/SBA-15}$. (f) STEM image and EDX mapping of a cross-sectional specimen of $200\text{TiO}_2\text{-1.5/SBA-15}$ prepared by focused ion beam milling.

In principle, when a hollow plug forms at the pore entrance of SBA-15, the straight tubular channels are converted to “ink-bottle” pores. The N_2 adsorption-desorption isotherms (ADI) of both SBA-15 and Co(salen)/SBA-15 are typical of type IV with an H1 hysteresis loop, which is indicative of a cylindrical pore structure (Figure 2a). As expected, the N_2 -ADI of $200\text{TiO}_2\text{-1.5/Co(salen)/SBA-15}$ are typical of type IV with an H2 hysteresis loop, which is indicative of an ink-bottle pore structure (Figure S1).^[14] A control experiment was also performed by depositing 200 cycles of TiO_2 in SBA-15 without

loading Co(salen) (200TiO₂-1.5/SBA-15). The N₂-ADI results also present a similar H2 hysteresis loop as that of 200TiO₂-1.5/Co(salen)/SBA-15 (Figure S6), confirming that the “ink-bottle” pore structure indeed resulted from the deposition of TiO₂ rather than from the loading of Co(salen).

The size of the pore entrance 200TiO₂-1.5/SBA-15 was also estimated using Co(salen) as a probe molecule in a dichloromethane (DCM) solution (Figure 2b). As expected, after treating the Co(salen) solution with 200TiO₂-1.5/SBA-15, the content of Co(salen) in the DCM remained nearly unchanged, indicating that the pore size at the entrance of 200TiO₂-1.5/SBA-15 was small enough to prevent the diffusion of Co(salen) into the channels. In contrast, the content of Co(salen) in DCM after treatment with SBA-15 dramatically decreased, suggesting that the pore entrance of SBA-15 was large enough to allow for the inward diffusion of Co(salen). This result further confirms that 200TiO₂-1.5/SBA-15 can be used as a suitable host material to entrap Co(salen).

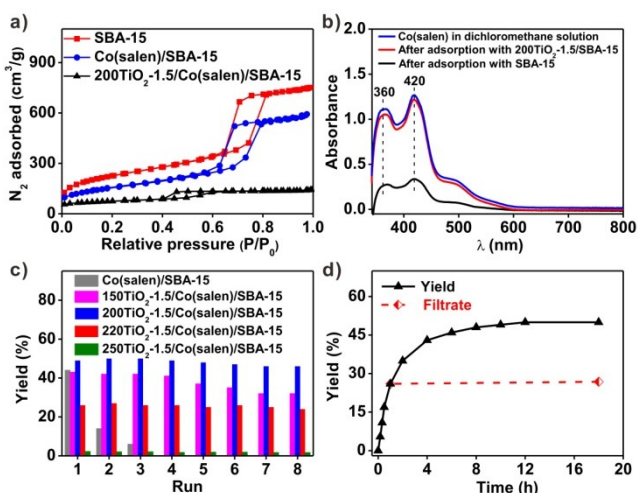


Figure 2. a) N₂ adsorption-desorption isotherms of SBA-15, Co(salen)/SBA-15 and the encapsulated catalyst 200TiO₂-1.5/Co(salen)/SBA-15. b) UV-vis spectra of Co(salen) dissolved in dichloromethane before and after treatment with SBA-15 and 200TiO₂-1.5/SBA-15. c) Activity and reusability of *m*TiO₂-1.5/Co(salen)/SBA-15 produced with different TiO₂ ALD cycle numbers for the hydration of propylene oxide. d) Kinetic study of the asymmetric hydration of propylene oxide over 200TiO₂-1.5/Co(salen)/SBA-15.

The hydrolytic kinetic resolution (HKR) of epoxides was used as a probe reaction for the encapsulated catalysts. The influence of the cycle number (*m*) on the catalytic performance was investigated for TiO₂ ALD with a fixed diffusion time (1.5 s) of TIP for *m*TiO₂-1.5/Co(salen)/SBA-15 catalysts (*m* = 150, 200, 220 and 250) since the size of pore entrance gradually decreases as the cycle numbers increase (Figure 2c, Table S1-S3). For Co(salen)/SBA-15 without encapsulation, the yield of diol dropped rapidly from 44% to 6% after 3 reaction runs due to the leaching of Co(salen), revealing a poor stability. The 150TiO₂-1.5/Co(salen)/SBA-15 provided a 43% yield of diol (for the first run). After 8 reaction runs, the yield reduced to 32%. This is due to the insufficient ALD cycle number, resulting in a pore size of the hollow plug larger than 0.8 nm and leaching of

some Co(salen) molecules during the recycling. In contrast, the 200TiO₂-1.5/Co(salen)/SBA-15 (0.59 wt% Co(salen)) exhibited a higher yield (>49%) than that of the 150TiO₂-1.5/Co(salen)/SBA-15 and the homogeneous reaction (using Co(salen) only, Table 1). After recycling, the yield and Co content very slightly reduced to 46% and 0.57 wt%, respectively, revealing an excellent stability. However, only a 26% diol yield was obtained for 220TiO₂-1.5/Co(salen)/SBA-15 in spite of the stable yield after recycling (24 wt%). According to the growth rate, 20 cycles of TiO₂ ALD (reducing 1 nm pore size) will completely close the pores of the hollow plugs (0.8 nm). Thus, the remaining activity should be ascribed to the original pores that had a size larger than the most probable pore size of 9.2 nm due to the pore size distribution of SBA-15 (Figure S1). Finally, when the cycle number was further increased to 250, the 250TiO₂-1.5/Co(salen)/SBA-15 shows no activity, revealing that all the pores were completely blocked (Figure S7). These results suggest that the 200TiO₂-1.5/Co(salen)/SBA-15 shows an optimized performance considering both the activity and stability. This matches well with the suitable pore size of the hollow plugs produced with 200 cycles of TiO₂ ALD, as revealed by TEM analysis (Figure 1c and 1d). For these *m*TiO₂-1.5/Co(salen)/SBA-15 catalysts, the enantioselectivity of all their diol products (including the recycling reactions) are 96~98%, similar to that of the homogeneous reaction, implying that the molecular structure or chirality of Co(salen) is well maintained after the encapsulation.

Figure 2d presents the kinetic plots of the hydration of propylene oxide over 200TiO₂-1.5/Co(salen)/SBA-15 to further confirm the successful encapsulation. The encapsulated catalyst was filtered off after the reaction was carried out for 1 h. The filtrate was continuously stirred for another 17 h, but the yield of the diol was almost the same as that measured at 1 h. In addition, the 200TiO₂-1.5/SBA-15 was evaluated, and it did not show any activity for the HKR reaction. Therefore, the encapsulated Co(salen) is indeed responsible for the catalytic reaction, and there is no apparent leaching of Co(salen). The influence of the local density of Co(salen) encapsulated in 200TiO₂-1.5/Co(salen)/SBA-15 was investigated to further reveal its advantages. When the Co content increased from 0.13 wt% to 0.65 wt%, the yield of diol increased sharply from 17% to 49% (Table 1, Table S4-S6). Correspondingly, the turnover frequency (TOF) increased from 48 h⁻¹ to 186 h⁻¹, which can be ascribed to the enhanced synergistic effect between the Co(salen) complexes.^[7b] The enhanced synergistic effect was further demonstrated by directly comparing the catalytic performance of 200TiO₂-1.5/Co(salen)/SBA-15 with the homogeneous reaction with Co(salen). The TOF of 200TiO₂-1.5/Co(salen)/SBA-15 (up to 186 h⁻¹) was higher than that of homogeneous Co(salen) (131 h⁻¹), because the local density of Co(salen) confined in the nanochannels of SBA-15 is much higher than that in the homogeneous system.

Generally, the ALD process in a nanochannel is governed by Knudsen diffusion.^[9b] According to the equation mentioned by Gordon et al.,^[15] the deposition depth depends on the diffusion time of the ALD precursors. Thus, the influence of diffusion time on the performance of the encapsulated catalyst was also investigated. The exposure times of 0 s and 8 s after 0.5 s pulse time were also applied for TIP, and the corresponding catalysts

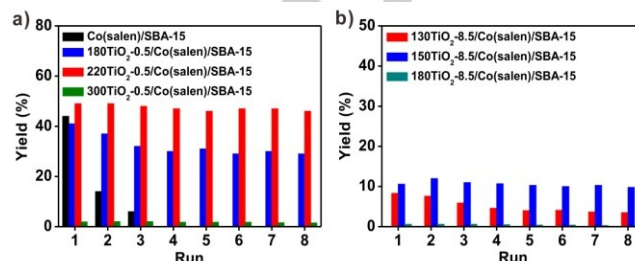
Table 1. The HKR of propylene oxide on homogeneous Co(salen) and encapsulated Co(salen) in mesoporous materials.^[a]

Catalyst	Co content (wt%) ^[b]	Diol yield (%)	Diol enantioselectivity (%)	TOF (h ⁻¹) ^[c]
Co(salen)	—	44	97	131
200TiO ₂ -1.5/SBA-15	—	N.D.	—	—
	0.13	17(14) ^[d]	97(96) ^[d]	48
	0.37	39(35) ^[d]	96(97) ^[d]	125
200TiO ₂ -1.5/Co(salen)/SBA-15	0.59	>49(47) ^[d]	98(98) ^[d]	186
	0.65	49(47) ^[d]	98(97) ^[d]	179
	80TiO ₂ -1.5/Co(salen)/SBA-15 (4.2 nm)	0.31	49(46) ^[d]	96(95) ^[d]
60TiO ₂ -1.5/Co(salen)/MCM-41 (3.2 nm)	0.29	48(44) ^[d]	96(98) ^[d]	116
80TiO ₂ -1.5/Co(salen)/SBA-16 (4.3 nm)	0.26	49(45) ^[d]	97(98) ^[d]	121

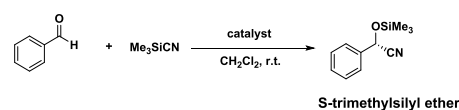
[a] Reactions were carried out with 0.55 equiv of H₂O and 0.2 mol% Co(salen) catalyst for 18 h. [b] Determined by ICP. [c] TOF is calculated according to the following equation: TOF = $N_{\text{converted propylene oxide}} / (N_{\text{Co(salen)}} \times t)$, where N denotes molar numbers, and t denotes reaction time (h). [d] The number in the bracket is the result after eight cycles of reaction.

were denoted as *m*TiO₂-0.5/Co(salen)/SBA-15 and *m*TiO₂-8.5/Co(salen)/SBA-15, respectively. Similarly, the number of ALD cycles was optimized in terms of the activity and stability. For a 0.5 s diffusion time, the optimized number of cycles is 220, and the produced catalyst 220TiO₂-0.5/Co(salen)/SBA-15 also shows good activity and stability (Figure 3a). It has a similar “ink bottle” pore structure as shown in the N₂-ADI analysis (Figure S8), which was further confirmed by EDX mapping, revealing a TiO₂ deposition depth of approximately 550 nm (Figure S9a). The shorter deposition depth is reasonable in terms of the shorter diffusion time of TIP. However, for an 8.5 s diffusion time, the optimized number of cycles is 150 (150TiO₂-8.5/Co(salen)/SBA-15). 150TiO₂-8.5/Co(salen)/SBA-15 has a very low activity despite its good stability (Figure 3b). The TiO₂ deposition depth reaches 5–6 μm (Figure S9b), which is consistent with the longer diffusion time (Scheme 1c). Obviously, the low activity resulted from the coverage of a majority of Co(salen) by TiO₂ and the limited diffusion of reactant molecules in the long channels with a too small pore size of 0.8 nm. Therefore, it is important to control the deposition depth of TiO₂ by choosing an appropriate diffusion time to optimize the stability and activity of the encapsulated catalyst. Note that the determined deposition depth are smaller than the simulated

values (for example, 4.5 μm for 1.5 s diffusion time at 0.1 torr TIP partial pressure).^[15] This can be ascribed to the specific deposition conditions including the deposition temperature, TIP partial pressure, flow rate of carrying gas, reactor structure, and so on.

**Figure 3.** Activity and reusability for the hydration of propylene oxide of *m*TiO₂-0.5/Co(salen)/SBA-15 (a) and *m*TiO₂-8.5/Co(salen)/SBA-15 (b) produced with different TiO₂ ALD cycle numbers.

This encapsulation strategy can also be applied to other ordered mesoporous materials and reactions due to the precise control of the pore size at the entrance. Table 1 and Figure S10 also show the catalytic performance of Co(salen) encapsulated in different mesoporous materials, including SBA-15 with a smaller pore size (4.2 nm), MCM-41 (3.2 nm), and SBA-16 (4.3 nm). All the encapsulated catalysts prepared with optimized TiO₂ ALD cycle numbers produced an increased yield of diol and excellent reusability compared to the homogeneous catalysts. Additionally, this strategy is feasible for the encapsulation of other metal complexes by ALD with optional encapsulating materials due to the extensive availability of various materials. For example, [(salen)Ti(μ-O)]₂ is encapsulated into SBA-15 by depositing Al₂O₃ via ALD (Table 2 and Figure S11). The encapsulated catalyst exhibited excellent activity and reusability for asymmetric cyanosilylation of carbonyl compounds.

Table 2. The asymmetric cyanosilylation of carbonyl compounds on 100Al₂O₃/[(salen)Ti(μ-O)]₂/SBA-15 and homogeneous [(salen)Ti(μ-O)]₂.^[a]

Catalyst	Ti content (wt%) ^[b]	Yield (%)	Enantioselectivity (%)
[(salen)Ti(μ-O)] ₂	—	>99	82
100Al ₂ O ₃ /[(salen)Ti(μ-O)] ₂ /SBA-15	0.11	96(94) ^[c]	81(80) ^[c]
	0.35	99(95) ^[c]	83(83) ^[c]
	0.52	>99(96) ^[c]	82(83) ^[c]

[a] Reactions were carried out under an argon atmosphere with 0.1 mol% Ti catalyst for 2 h. [b] Determined by ICP. [c] The number in the bracket is the results after 6 cycles of reaction.

In conclusion, we have demonstrated for the first time that ALD can be applied for the encapsulation of homogeneous

catalysts in a series of mesoporous materials. This was realized by depositing metal oxides at/near the pore entrance via controlling the diffusion time of the precursors to form a hollow plug. Its pore sizes can be precisely tailored at the sub-nanometer scale by controlling the ALD cycle number. Typically, by accommodating Co(salen) and [(salen)Ti(μ -O)]₂ in SBA-15, the produced catalysts exhibit excellent activity and reusability in the HKR of the epoxides and asymmetric cyanosilylation of carbonyl compounds, respectively. The encapsulated catalysts can be easily recycled by filtration with very slight loss of catalytic activity. This is a general strategy that can be easily extended to the development of many other solid catalysts for the sustainable production of chemicals and pharmaceuticals in industry.

Acknowledgements

We appreciate the financial support from the National Natural Science Foundation of China (21403271 and 21673269) and Youth Innovation Promotion Association CAS (2017204).

Keywords: encapsulation • hollow plugs • atomic layer deposition • asymmetric catalysis • mesoporous materials

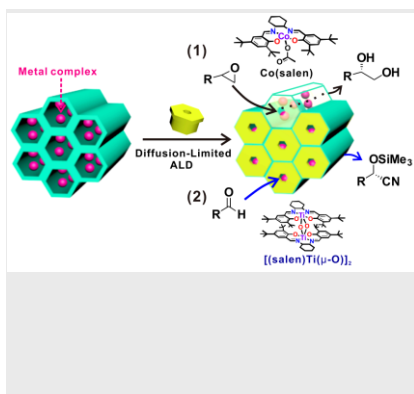
- [1] K. Renggli, P. Baumann, K. Langowska, O. Onaca, N. Bruns, W. Meier, *Adv. Fun. Mater.* **2011**, 21, 1241-1259.
- [2] a) M. J. Monteiro, *Macromolecules* **2010**, 43, 1159-1168; b) T. H. Tran-Thi, R. Dagnelie, S. Crunaire, L. Nicole, *Chem. Soc. Rev.* **2011**, 40, 621-639; c) O. Onaca-Fischer, J. Liu, M. Inglin, C. G. Palivan, *Curr. Pharm. Des.* **2012**, 18, 2622-2643; d) J. Lee, S. M. Kim, I. S. Lee, *Nano Today* **2014**, 9, 631-667.
- [3] a) D. Shchukin, D. Sviridov, *J. Photoch. Photobiol. C* **2006**, 7, 23-39; b) Z. C. Zhang, B. Xu, X. Wang, *Chem. Soc. Rev.* **2014**, 43, 7870-7886.
- [4] a) Q. Yang, D. Han, H. Yang, C. Li, *Chem. Asian J.* **2008**, 3, 1214-1229; b) M. Shakeri, R. J. M. K. Gebbink, P. E. d. Jongh, K. P. d. Jong, *Angew. Chem.* **2013**, 125, 11054-11057; *Angew. Chem. Int. Ed.* **2013**, 52, 10854-10857.
- [5] A. Corma, H. Garcia, *Eur. J. Inorg. Chem.* **2004**, 2004, 1143-1164.
- [6] a) F. Algarra, M. A. Esteves, V. Forne, H. Garc, J. Primoa, *New J. Chem.* **1998**, 333-338; b) J. He, X. Li, D. G. Evans, X. Duan, C. Li, *J. Mol. Catal. B: Enzym.* **2000**, 11, 45-53; c) H. Ma, J. He, D. G. Evans, X. Duan, *J. Mol. Catal. B: Enzym.* **2004**, 30, 209-217; d) J. He, Z. Song, H. Ma, L. Yang, C. Guo, *J. Mater. Chem.* **2006**, 16, 4307-4315.
- [7] a) H. Yang, J. Li, J. Yang, Z. Liu, Q. Yang, C. Li, *Chem. Commun.* **2007**, 1086-1088; b) H. Yang, L. Zhang, L. Zhong, Q. Yang, C. Li, *Angew. Chem.* **2007**, 119, 6985-6989; *Angew. Chem. Int. Ed.* **2007**, 46, 6861-6865; c) H. Yang, L. Zhang, P. Wang, Q. Yang, C. Li, *Green Chem.* **2009**, 11, 257-264; d) B. Li, S. Bai, P. Wang, H. Yang, Q. Yang, C. Li, *Phys. Chem. Chem. Phys.* **2011**, 13, 2504-2511; e) B. Li, S. Bai, X. Wang, M. Zhong, Q. Yang, C. Li, *Angew. Chem.* **2012**, 124, 11685-11689; *Angew. Chem. Int. Ed.* **2012**, 51, 11517-11521; f) J. Liu, G. Lan, J. Peng, Y. Li, C. Li, Q. Yang, *Chem. Commun.* **2013**, 49, 9558-9560; g) J. Peng, X. Wang, X. Zhang, S. Bai, Y. Zhao, C. Li, Q. Yang, *Catal. Sci. Technol.* **2015**, 5, 666-672.
- [8] S. M. L. d. Santos, K. A. B. Nogueira, M. d. S. Gama, J. D. F. Lima, Ivanildo José da Silva Júnior, D. C. S. d. Azevedo, *Micropor. Mesopor. Mat.* **2013**, 180, 284-292.
- [9] a) S. M. George, *Chem. Rev.* **2010**, 110, 111-131; b) C. Detavernier, J. Dendooven, S. P. Sree, K. F. Ludwig, J. A. Martens, *Chem. Soc. Rev.* **2011**, 40, 5242-5253; c) N. P. Dasgupta, H.-B.-R. Lee, S. F. Bent, P. S. Weiss, *Chem. Mater.* **2016**, 28, 1943-1947.
- [10] a) F. Li, L. Li, X. Liao, Y. Wang, *J. Membr. Sci.* **2011**, 385-386, 1-9; b) V. Romero, V. Vega, J. García, R. Zierold, K. Nielsch, V. M. Prida, B. Hernando, J. Benavente, *ACS Appl. Mater. Interfaces* **2013**, 5, 3556-3564; c) C. Wang, D. Kong, Q. Chen, J. Xue, *Front. Mater. Sci.* **2013**, 7, 335-349.
- [11] a) Z. Gao, M. Dong, G. Wang, P. Sheng, Z. Wu, H. Yang, B. Zhang, G. Wang, J. Wang, Y. Qin, *Angew. Chem.* **2015**, 127, 9134-9138; *Angew. Chem. Int. Ed.* **2015**, 54, 9006-9010; b) B. Zhang, Y. Chen, J. Li, E. Pippel, H. Yang, Z. Gao, Y. Qin, *ACS Catal.* **2015**, 5, 5567-5573; c) H. Ge, B. Zhang, X. Gu, H. Liang, H. Yang, Z. Gao, J. Wang, Y. Qin, *Angew. Chem.* **2016**, 128, 7197-7201; *Angew. Chem. Int. Ed.* **2016**, 55, 7081-7085; d) B. Zhang, X.-W. Guo, H. Liang, H. Ge, X. Gu, S. Chen, H. Yang, Y. Qin, *ACS Catal.* **2016**, 6, 6560-6566; e) M. Wang, Z. Gao, B. Zhang, H. Yang, Y. Qiao, S. Chen, H. Ge, J. Zhang, Y. Qin, *Chem. Eur. J.* **2016**, 22, 8438-8443; f) Y. Li, S. Zhao, Q. Hu, Z. Gao, Y. Liu, J. Zhang, Y. Qin, *Catal. Sci. Technol.* **2017**, 7, 2032-2038; g) J. Zhang, Z. Yu, Z. Gao, H. Ge, S. Zhao, C. Chen, S. Chen, X. Tong, M. Wang, Z. Zheng, Y. Qin, *Angew. Chem.* **2017**, 129, 834-838; *Angew. Chem. Int. Ed.* **2017**, 56, 816-820; h) H. Liang, B. Zhang, H. Ge, X. Gu, S. Zhang, Y. Qin, *ACS Catal.* **2017**, 7, 6567-6572; i) B. Zhang, X. Gu, H. Liang, H. Ge, H. Yang, Y. Qin, *J. Fuel. Chem. Tech.* **2017**, 45, 714-722.
- [12] a) M. D. Groner, F. H. Fabreguette, J. W. Elam, S. M. George, *Chem. Mater.* **2004**, 16, 639-645; b) M. Knez, A. Kadri, C. Wege, U. Gosele, H. Jeske, K. Nielsch, *Nano Lett* **2006**, 6, 1172-1177; c) J. S. King, E. Graugnard, O. M. Roche, D. N. Sharp, J. Scrimgeour, R. G. Denning, A. J. Turberfield, C. J. Summers, *Adv. Mater.* **2006**, 18, 1561-1565; d) M. Knez, K. Nielsch, L. Niinistö, *Adv. Mater.* **2007**, 19, 3425-3438.
- [13] C. A. Bessel, D. R. Rolison, *J. Phys. Chem. B* **1997**, 101, 1148-1157.
- [14] a) P. V. D. Voort, P. I. Ravikovitch, K. P. D. Jong, M. Benjelloun, E. V. Bavel, A. H. Janssen, A. V. Neimark, B. M. Weckhuysen, E. F. Vansant, *J. Phys. Chem. B* **2002**, 106, 5873-5877; b) A. Vishnyakov, A. V. Neimark, *Langmuir* **2003**, 19, 3240-3247.
- [15] R. G. Gordon, D. Hausmann, E. Kim, J. Shepard, *Chem. Vap. Dep.* **2003**, 9, 73-78.

Entry for the Table of Contents (Please choose one layout)

Layout 1:

COMMUNICATION

Metal complexes have been successfully encapsulated in mesoporous materials by atomic layer deposition of metal oxides at/near the pore entrance to form a hollow plug via controlling the diffusion time of the precursors.



Shufang Zhang, Bin Zhang,* Haojie Liang, Yejun Liu, Yan Qiao, Yong Qin*

Page No. – Page No.

Encapsulation of Homogeneous Catalysts in Mesoporous Materials Using Diffusion-Limited Atomic Layer Deposition